International Journal of Network Dynamics and Intelligence Scilight

Article

Probability-Guaranteed Consensus Control for Nonlinear Multi-Agent Systems Under Bit Flips

Shuo Yuan, Lifeng Ma, and Chen Gao *

School of Automation, Nanjing University of Science and Technology, Nanjing 210094, China
* Correspondence: chengao@njust.edu.cn

Received: 26 May 2025
Accepted: 2 July 2025
Published: 18 September 2025

Abstract: In this paper, the consensus control problem for discrete multi-agent systems is investigated in the presence of bit flips. First, a bit-rate allocation model with a finite number of bytes, together with an encoding-decoding scheme, is constructed to depict the constraints of bandwidth limitations. Then, a Bernoulli distribution is introduced to characterize the stochastic bit flips, while the impacts of bit flips on encoding-decoding processes are systematically analyzed by leveraging stochastic analysis theory. A novel control framework is proposed within a probabilistic ellipsoidal constraint, ensuring robustness against bit errors and nonlinear dynamics. By virtue of linear matrix inequalities (LMIs), sufficient conditions for the controller are derived to ensure probability-guaranteed consensus. Finally, the effectiveness of the designed controller is illustrated via numerical simulations, confirming its practical applicability in networked control systems with unreliable communication channels.

Keywords: nonlinear multi-agent systems; probability-guaranteed consensus control; uniform quantization; bit flips

1. Introduction

Multi-agent systems (MASs) consist of multiple autonomous agents that cooperate and communicate to achieve a global objective. Ensuring consistency within MASs is a key challenge, as agents must align their actions and states despite having limited local information. Consensus control in MASs involves designing strategies that enable agents to synchronize or agree on certain parameters, such as position and velocity, despite their decentralized nature [1–9]. This coordination is crucial for tasks in dynamic and uncertain environments, ensuring robust performance and resilience to faults or disturbances. Therefore, consensus control plays a vital role in the scalability and adaptability of MASs in real-world applications [10, 11].

In engineering practice, MASs are often subjected to stochastic disturbances such as communication noise, data loss, and uncertainties in dynamic environments[12−14]. Traditional control methods typically assume a deterministic system model and require that the system states strictly reach or maintain the desired values. However, in stochastic environments, such strict requirements are often unrealistic and can lead to significant design challenges and increased computational complexity [15, 16]. The probability-guaranteed control design reformulates control problems by aiming to achieve the desired system behavior with a certain probability under random conditions. Unlike traditional deterministic designs, the probability-guaranteed design relaxes the performance requirements by specifying that the system should meet the expected behavior within a given probability range, thus avoiding overly stringent constraints. This approach not only makes the design more feasible in uncertain environments but also provides greater flexibility to optimize other performance metrics. For example, in Ref. [17], a self-triggered model predictive control protocol has been proposed for MASs with uncertainty, transforming probability constraints into deterministic ones using Cantelli's inequality, ensuring system stability and recursive feasibility. A distributed stochastic MPC approach has been introduced for dynamically coupled linear systems under cumulative disturbances, ensuring recursive feasibility and meeting probability constraints through a data-driven method [18]. A data-driven robust predictive control algorithm has been developed for stochastic systems, achieving a higher probability of constraint

satisfaction compared to traditional methods [19].

Network resources in MASs are often limited due to constraints such as network bandwidth, transmission bit rates, and energy availability. Encoding-decoding mechanisms provide an effective approach to address these limitations by mapping continuous or high-resolution information into finite-bit digital signals. In this context, the privacy protection in distributed consensus control has been examined for second-order MASs with limited communication channel capacity and partial state observability [20]. Specifically, quantization techniques have been applied to address communication constraints, a dynamic encoding-decoding strategy has been developed for estimating the real-valued states of neighboring agents, and in addition, a differentially private consensus algorithm has been proposed to safeguard privacy. In Ref. [21], the synchronization issue has been investigated for linear MASs with unmeasurable states under limited communication rates and switching topologies, where a quantized observer-based coding-decoding scheme as well as a control protocol has been introduced based on the principle of deterministic equivalence. Moreover, the leader-follower consensus problem has been addressed for discrete nonlinear MASs under switching topologies and limited bandwidth in [22], where a distributed feedback controller has been proposed to minimize data transmission at each time step while ensuring the quantizer does not saturate.

In this paper, the probability-guaranteed consensus control problem is investigated for a class of time-varying stochastic nonlinear MASs. The proposed system model integrates stochastic nonlinear dynamics and addresses practical challenges such as unknown noise and sensor saturation. The main contributions are as follows: 1) a novel probability-guaranteed consensus criterion is proposed to address stochastic nonlinear dynamics and bit flips; 2) a comprehensive model is developed by integrating bit-rate constraints, encoding-decoding mechanisms, and sensor saturation effects; and 3) a mathematical model is formulated to characterize bit flips in binary codewords, enabling quantitative evaluation of their impacts on decoding accuracy and control performance.

Notation: $\mathbb{R}$ denotes the set of real numbers, and $\mathbb{R}^n$ represents the n-dimensional Euclidean space. $\mathbb{R}^{m\times n}$ stands for the set of all $m\times n$ real matrices. $\mathbf{1}_n$ denotes an n-dimensional column vector with all entries equal to 1, and I_n represents the n-dimensional identity matrix. The notation $\mathrm{col}_m\{b_i\}$ refers to the column vector $[b_1^{\mathrm{T}}, b_2^{\mathrm{T}}, \cdots, b_m^{\mathrm{T}}]^{\mathrm{T}}$. $\mathrm{diag}\{\cdots\}$ indicates a block diagonal matrix, and $\mathrm{diag}_m\{A_i\}$ represents the block diagonal matrix $\mathrm{diag}\{A_1, A_2, \cdots, A_m\}$. $A>0$ (or $A\geqslant 0$) means that the matrix A is positive definite (or positive semi-definite). The symbol $\otimes$ is used to denote the Kronecker product of matrices. The symbol $*$ refers to the symmetric block in a symmetric block matrix. $\mathbb{E}\{x\}$ represents the mathematical expectation of the random variable x, and $\mathrm{Var}\{x\}$ denotes the variance of x. $\mathbb{P}\{Q\}$ is the probability of event Q occurring. $\mathcal{B}(\cdot)$ and $\mathcal{B}^{-1}(\cdot)$ represent the binaryization and inverse binaryization functions, respectively. $\mathrm{sign}(\cdot)$ denotes the sign function.

2. Problem Formulation

Consider an MAS consisting of N agents. The communication topology between agents is represented by a fixed undirected graph $\mathfrak{G}=(\mathfrak{V},\mathfrak{E},\mathfrak{H})$, where $\mathfrak{V}=\{1,2,\cdots,N\}$ is the set of nodes, $\mathfrak{E}$ is the set of edges, and $\mathfrak{H}=[h_{ij}]\in\mathbb{R}^{N\times N}$ is a symmetric weighted adjacency matrix. If there is a communication link between agent i and agent j, i.e., edge $(i,j)\in\mathfrak{E}$, then $h_{ij}>0$; otherwise, $h_{ij}=0$. The agents are assumed to have no self-connections, meaning that $h_{ii}=0$. In addition, the in-degree of node i is defined as $\deg_{\mathrm{in}}^i \triangleq \sum_{j=1}^{N} h_{ij}$, the in-degree matrix is $\mathfrak{D}\triangleq \mathrm{diag}_N\{\deg_{\mathrm{in}}^i\}$, and the topology matrix is $\mathcal{H}\triangleq\mathfrak{H}-\mathfrak{D}$.

2.1. System Model

Consider a class of discrete time-varying MASs represented as follows:

$$\begin{cases} x_{i,k+1}=A_k x_{i,k}+B_k u_{i,k}+D_k\omega_{i,k}+f(x_{i,k}) \\ y_{i,k}=\mathcal{G}(C_k x_{i,k})+E_k v_{i,k} \end{cases} \tag{1}$$

where $i\in\mathfrak{V}$, $x_{i,k}\in\mathbb{R}^n$, $u_{i,k}\in\mathbb{R}^p$ and $y_{i,k}\in\mathbb{R}^m$ represent the state, control input and measurement output of agent i, respectively. The process noise $\omega_{i,k}\in\mathbb{R}^w$ and measurement noise $v_{i,k}\in\mathbb{R}^v$ are also considered. The time-varying matrices A_k, B_k, C_k, D_k and E_k are known and appropriately dimensioned. Let $f_{i,k}\triangleq f(x_{i,k})$ denote a nonlinear function of the state. The stochastic nonlinear function $f_{i,k}$ possesses the following statistical properties:

$$\begin{aligned} &\mathbb{E}\{f_{i,k}|x_{i,k}\}=0, \\ &\mathbb{E}\{f_{i,k}f_{j,k}^{\mathrm{T}}|x_{i,k}\}=0, \quad i\neq j \\ &\mathbb{E}\{f_{i,k}f_{i,k}^{\mathrm{T}}|x_{i,k}\}\leqslant\sum_{l=1}^{s}\Omega_{il,k}(x_{i,k}^{\mathrm{T}}\Gamma_{il,k}x_{i,k}) \end{aligned} \tag{2}$$

where $s\geqslant 0$ is a known integer, $\Omega_{il,k}\geqslant 0$ and $\Gamma_{il,k}\geqslant 0$ are known matrices with compatible dimensions. The

unknown but bounded noises $\omega_{i,k}$ and $v_{i,k}$ are confined within ellipsoids $\mathcal{W}_{i,k}$ and $\mathcal{V}_{i,k}$ defined as:

$$\begin{aligned} \omega_{i,k} \in \mathcal{W}_{i,k} &\triangleq \left\{\omega_{i,k} : \omega_{i,k}^{\mathrm{T}} W_{i,k}^{-1} \omega_{i,k} \leqslant 1\right\}, \\ v_{i,k} \in \mathcal{V}_{i,k} &\triangleq \left\{v_{i,k} : v_{i,k}^{\mathrm{T}} V_{i,k}^{-1} v_{i,k} \leqslant 1\right\}. \end{aligned} \tag{3}$$

where $W_{i,k} > 0$ and $V_{i,k} > 0$ are compatible matrices.

Definition 1: Given appropriately dimensioned matrices $\mathcal{T}_1$ and $\mathcal{T}_2$ such that $\mathcal{T}_2 - \mathcal{T}_1 > 0$. If the following condition holds:

$$(\mathfrak{h}(x) - \mathcal{T}_1 x)^{\mathrm{T}} (\mathfrak{h}(x) - \mathcal{T}_2 x) \leqslant 0, \tag{4}$$

then $\mathfrak{h}(\cdot)$ is called a sector-bounded nonlinear function and belongs to the interval $[\mathcal{T}_1, \mathcal{T}_2]$.

Since sensors have a limited measurement range, when the parameter being measured exceeds the sensor's range, saturation occurs. The saturation function $\mathcal{G}(\cdot)$ is defined as follows:

$$\mathcal{G}(\eta_{i,k}) \triangleq [\mathcal{G}(\eta_{i,k}^{(1)})\ \mathcal{G}(\eta_{i,k}^{(2)})\ \cdots\ \mathcal{G}(\eta_{i,k}^{(m)})]^{\mathrm{T}} \tag{5}$$

where $\mathcal{G}(\eta_{i,k}^{(l)}) = \operatorname{sign}(\eta_{i,k}^{(l)}) \min\{\mathfrak{M}_i^{(l)}, |\eta_{i,k}^{(l)}|\}$ $(l \in \{1, 2, \cdots, m\})$, and $\mathfrak{M}_i^{(l)} > 0$ is the value of the saturation boundary.

It is known that for appropriately dimensioned diagonal matrices T_1 and T_2 satisfying $0 \leqslant T_1 < I_m \leqslant T_2$, the saturation function $\mathcal{G}(C_k x_{i,k})$ can be transformed into the following form:

$$\mathcal{G}(C_k x_{i,k}) = T_1 C_k x_{i,k} + h(C_k x_{i,k}) \tag{6}$$

where $h(C_k x_{i,k})$ is a sector-bounded nonlinear function that belongs to the interval $[0, T]$, with $T = T_2 - T_1$. The function $h(C_k x_{i,k})$ satisfies:

$$h^{\mathrm{T}}(C_k x_{i,k}) \left(h(C_k x_{i,k}) - T C_k x_{i,k}\right) \leqslant 0. \tag{7}$$

2.2. Bit-rate Constraint

In practical wireless communication networks, the communication resources available to agents are often limited due to network bandwidth. The available bandwidth determines the bit-rate, which refers to the amount of data that can be transmitted per instance. In such cases, transmitting large volumes of data can lead to network congestion or prolonged encoding and decoding times, which negatively impacts the control performance of MASs. Therefore, studying the consensus control problem of MASs under bit-rate constraints is of considerable practical significance.

Based on the above background, we considers the scenario where agent communication is subject to bit-rate constraints. Specifically, agent i uses binary signals to transmit codewords, and the length of each codeword at each time is R_i bits.The encoder encodes each of the m components of the input signal, and the m codewords together form the content of the data payload. To ensure the optimal utilization of available bandwidth and the efficient transmission of data, agent i allocates Y_i bits to the m components, satisfying the Equation

$$R_i = m Y_i. \tag{8}$$

2.3. Encoding-Decoding Mechanism

In what follows, a uniform-quantizers-based communication mechanism is introduced for each agent. The quantizer $Q_i(\cdot)$ is defined as follows:

$$Q_i(\eta) = \begin{bmatrix} q_i(\eta^{(1)}) & q_i(\eta^{(2)}) & \cdots & q_i(\eta^{(m)}) \end{bmatrix}^{\mathrm{T}} \tag{9}$$

where $\eta \in \mathbb{R}^m$ is the input signal to the quantizer, and the quantization function $q_i(\eta^{(\iota)})$ for each component $(\iota = 1, 2, \cdots, m)$ is as follows:

$$q_i\left(\eta^{(\iota)}\right) = \begin{cases} -M_i, & \text{if}\, \eta^{(\iota)} \in (-\infty, -M_i) \\ -M_i + \dfrac{(2\beta_i - 1) M_i}{\alpha_i}, & \text{if}\, \eta^{(\iota)} \in R_{\beta_i, i} \\ M_i, & \text{if}\, \eta^{(\iota)} \in [M_i, \infty) \end{cases} \tag{10}$$

where the quantization range $[-M_i, M_i)$ is divided into α_i intervals, denoted as $R_{\beta_i,i} \triangleq \left[-M_i + \dfrac{2(\beta_i - 1) M_i}{\alpha_i}, -M_i + \dfrac{2\beta_i M_i}{\alpha_i}\right)$, where β_i corresponds to the quantization level of $\eta^{(\iota)}$, with $\beta_i = 1, 2, \cdots, \alpha_i$. A diagram of the quantization process is shown in Figure 1.

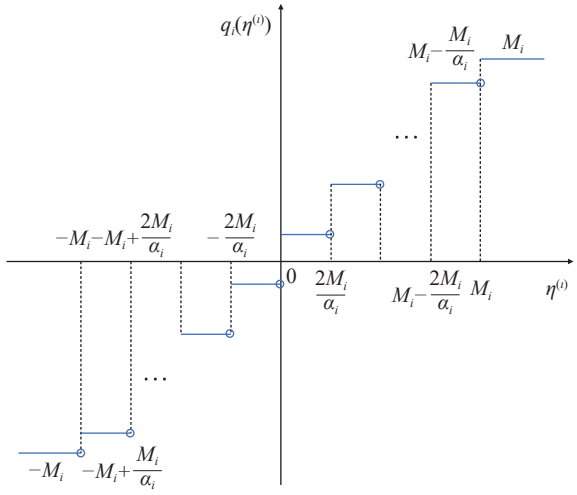

Figure 1. Quantification Diagram.

The quantization error is defined as $e_{i,k} \triangleq y_{i,k} - Q_i(y_{i,k})$. From Equation (10), we can derive the following inequality:

$$|e_{i,k}^{(\iota)}| \leqslant \frac{M_i}{\alpha_i}, \quad \iota = 1, 2, \cdots, m. \tag{11}$$

Next, the encoder and decoder are designed one by one.

Encoder:

$$\phi_{i,k} = \frac{\alpha_i(Q_i(y_{i,k}) + \tilde{M}_i) - \tilde{M}_i}{2M_i} \tag{12}$$

where $\phi_{i,k}$ represents the encoder's output, and α_i and M_i are the parameters related to the quantizer in Equation (10). Additionally, $\tilde{M}_i \triangleq M_i \mathbf{1}_m$. The encoder maps the m quantization levels corresponding to the components of $y_{i,k}$ into codewords of mY_i bits each. Considering the bit rate constraint in Equation (8), we have

$$\alpha_i = 2^{Y_i}. \tag{13}$$

Decoder:

$$\tilde{y}_{i,k} = -\tilde{M}_i + \frac{(2\phi_{i,k} + 1)M_i}{\alpha_i}. \tag{14}$$

where $\tilde{y}_{i,k}$ represents the output of the decoder. By substituting Equation (12) into the decoding process defined in Equation (14), we can straightforwardly deduce that $\tilde{y}_{i,k} = Q_i(y_{i,k})$.

2.4. Bit Flips

In engineering practice, the output of the encoder is typically transmitted through a wireless digital communication network in the form of binary codewords. However, during transmission, due to factors such as channel noise and multi-user interference, bit flips may occur. This refers to the phenomenon where certain bits in the binary codeword undergo a $0-1$ flip. Such bit flips not only reduce decoding accuracy but may also have a significant negative impact on the system's control performance. Therefore, investigating the issue of bit flips under encoding and decoding mechanisms holds both theoretical and practical importance.

To simplify the problem description, we first consider the case where the dimension of $y_{i,k}$ is $m = 1$. In this case, both the encoder output $\phi_{i,k}$ and the decoder output $\tilde{y}_{i,k}$ have a dimension of 1.

Let the binary codeword of $\phi_{i,k}$ be:

$$\phi_{i,k}^{bin} = \mathcal{B}(\phi_{i,k}) \triangleq \langle b_{ik,Y_i}, \cdots, b_{ik,2}, b_{ik,1} \rangle \tag{15}$$

where $b_{ik,s} \in \{0, 1\}$ represents the s-th bit of $\phi_{i,k}^{bin}$ from the least significant bit to the most significant bit, with $s \in \{1, 2, \cdots, Y_i\}$.

As shown in Figure 2, after transmission through an unstable communication network, the bit values of each position in $\phi_{i,k}^{bin}$ may undergo bit flips with a certain probability. The transmitted codeword is denoted as:

$$\hat{\phi}_{i,k}^{bin} \triangleq \langle \hat{b}_{ik,Y_i}, \cdots, \hat{b}_{ik,2}, \hat{b}_{ik,1} \rangle \tag{16}$$

where $\hat{b}_{ik,s} \in \{0,1\}$ represents the s-th bit of $\hat{\phi}_{i,k}^{bin}$ from the least significant bit to the most significant bit, with $s \in \{1,2,\cdots,Y_i\}$. The bit value $\hat{b}_{ik,s}$ satisfies:

$$\hat{b}_{ik,s} = p_{i,s}(1-b_{ik,s}) + (1-p_{i,s})b_{ik,s} \tag{17}$$

where the random variable $p_{i,s}$ follows a Bernoulli distribution with parameter $\bar{p}_i \in (0,1)$. Additionally, it satisfies $\mathbb{E}\{p_{i,s_1}p_{j,s_2}\} = \mathbb{E}\{p_{i,s_1}p_{j,s_2}\}, i \neq j, s_1, s_2 \in \{1,2,\cdots,Y_i\}$. The variable $p_{i,s}$ describes whether a bit flip occurs in $b_{ik,s}$, as expressed below:

$$\begin{cases} \mathbb{P}\{p_{i,s}=1\} = \bar{p}_i, & b_{ik,s} \text{ flips} \\ \mathbb{P}\{p_{i,s}=0\} = 1-\bar{p}_i, & b_{ik,s} \text{ remains unchanged} \end{cases} \tag{18}$$

Define $\hat{\phi}_{i,k} = \mathcal{B}^{-1}(\hat{\phi}_{i,k}^{bin})$. The encoder performs inverse binary conversion on the received codeword $\hat{\phi}_{i,k}^{bin}$ to obtain $\hat{\phi}_{i,k}$, which is then substituted into Equation (14) to determine the actual output of the decoder.

$$\begin{aligned} \hat{y}_{i,k} &= -M_i + \frac{\left(2\hat{\phi}_{i,k}+1\right)M_i}{\alpha_i} \\ &= -M_i + \frac{\left(2\sum_{s=1}^{Y_i}\hat{b}_{ik,s}2^{s-1}+1\right)M_i}{\alpha_i} \\ &= -M_i + \frac{\left(\sum_{s=1}^{Y_i}\hat{b}_{ik,s}2^{s}+1\right)M_i}{\alpha_i}. \end{aligned} \tag{19}$$

Based on the above bit flip model, this chapter presents the following lemma:

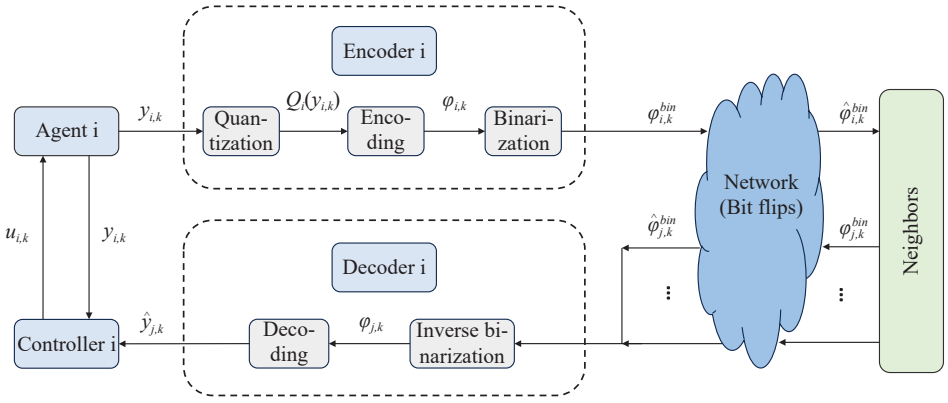

Figure 2. System Communication Block Diagram

Lemma 1: For the coding and decoding mechanisms given by (12) and (14), after transmission through a communication network with a bit flip probability of $\bar{p}_i$, the decoded value $\hat{y}_{i,k}$ has the following statistical properties:

$$\begin{aligned} &\mathbb{E}\{\hat{y}_{i,k}\} = (1-2\bar{p}_i)q(y_{i,k}), \\ &\mathrm{Var}\{\hat{y}_{i,k}\} = \frac{4}{3}\bar{p}_i(1-\bar{p}_i)\frac{M_i^2(2^{2Y_i}-1)}{2^{2Y_i}}. \end{aligned} \tag{20}$$

Extend the above conclusion to the case where the dimension of $y_{i,k}$ is $m \geqslant 1$. In this case, agent i encodes the m components of the dimension of $y_{i,k}$ separately, with the encoder input and output given by

$$\begin{aligned} y_{i,k} &= \left[\begin{array}{cccc} y_{i,k}^{(1)} & y_{i,k}^{(2)} & \cdots & y_{i,k}^{(m)} \end{array}\right]^{\mathrm{T}}, \\ \phi_{i,k} &= \left[\begin{array}{cccc} \phi_{i,k}^{(1)} & \phi_{i,k}^{(2)} & \cdots & \phi_{i,k}^{(m)} \end{array}\right]^{\mathrm{T}}. \end{aligned} \tag{21}$$

Correspondingly, the encoder's received and decoded values are

$$\begin{aligned} \hat{\phi}_{i,k} &= \left[\begin{array}{cccc} \hat{\phi}_{i,k}^{(1)} & \hat{\phi}_{i,k}^{(2)} & \cdots & \hat{\phi}_{i,k}^{(m)} \end{array}\right]^{\mathrm{T}}, \\ \hat{y}_{i,k} &= \left[\begin{array}{cccc} \hat{y}_{i,k}^{(1)} & \hat{y}_{i,k}^{(2)} & \cdots & \hat{y}_{i,k}^{(m)} \end{array}\right]^{\mathrm{T}}. \end{aligned} \tag{22}$$

Based on Lemma 1, it is obvious that

$$\mathbb{E}\{\hat{y}_{i,k}\} = (1-2\bar{p}_i)Q(y_{i,k}), \tag{23}$$

$$\mathrm{Var}\{\hat{y}_{i,k}^{(\iota)}\} = \frac{4}{3}\bar{p}_i(1-\bar{p}_i)\frac{M_i^2(2^{2Y_i}-1)}{2^{2Y_i}}, \quad \iota \in \{1,2,\cdots,m\}. \tag{24}$$

Define

$$\lambda_i \triangleq \frac{4}{3}\bar{p}_i(1-\bar{p}_i)\frac{M_i^2(2^{2Y_i}-1)}{2^{2Y_i}}. \tag{25}$$

Based on the above statistical properties, $\hat{y}_{i,k}$ can be expressed in the following form:

$$\hat{y}_{i,k} = (1-2\bar{p}_i)Q(y_{i,k}) + \gamma_{i,k} \tag{26}$$

where $\gamma_{i,k} \triangleq \begin{bmatrix} \gamma_{i,k}^{(1)} & \gamma_{i,k}^{(2)} & \cdots & \gamma_{i,k}^{(m)} \end{bmatrix}^{\mathrm{T}}$, and $\gamma_{i,k}^{(\iota)}$ is a random variable with zero mean and variance λ_i, $\iota \in \{1, 2,\cdots,m\}$.

2.5. Design Objective

The control protocol of the agents is constructed as follows:

$$u_{i,k} = K_k \sum_{j=1}^{N} h_{ij}(\hat{y}_{j,k} - y_{i,k}) \triangleq K_k \sum_{j=1}^{N} h_{ij}\chi_{i,k} \tag{27}$$

where K_k is the feedback control gain to be designed.

Substituting (27) into (1), we obtain:

$$x_{k+1} = \tilde{A}_k x_k + \tilde{B}_k \chi_k + \mathcal{D}_k \omega_k + f_k \tag{28}$$

where

$$\begin{aligned} &x_k \triangleq \mathrm{col}_N\{x_{i,k}\}, \quad \chi_k \triangleq \mathrm{col}_N\{\chi_{i,k}\}, \quad \omega_k \triangleq \mathrm{col}_N\{\omega_{i,k}\}, \\ &\tilde{A}_k \triangleq I_N \otimes A_k, \quad \tilde{K}_k \triangleq B_k K_k, \quad \tilde{B}_k \triangleq I_N \otimes \tilde{K}_k, \\ &\mathcal{D}_k \triangleq I_N \otimes D_k, \quad f_k \triangleq \mathrm{col}_N\{f_{i,k}\}. \end{aligned}$$

Define the average state of N agents as

$$\bar{x}_k \triangleq \mathbb{E}\left\{\frac{1}{N}\sum_{i=1}^{N} x_{i,k}\right\} = \mathbb{E}\left\{\frac{1}{N}(\mathbf{1}_N^{\mathrm{T}} \otimes I_n)x_k\right\}. \tag{29}$$

Combining (28), we can obtain

$$\bar{x}_{k+1} = \mathbb{E}\left\{\frac{1}{N}(\mathbf{1}_N^{\mathrm{T}} \otimes I_n)x_{k+1}\right\} = A_k\bar{x}_k + \frac{1}{N}\left(\mathbf{1}_N^{\mathrm{T}} \otimes \tilde{K}_k\right)\chi_k. \tag{30}$$

Definition 2: The ellipsoid $\mathcal{Q}(c, \mathfrak{C}) \in \mathbb{R}^n$ is defined as follows:

$$\mathcal{Q}(c, \mathfrak{C}) \triangleq \left\{x \in \mathbb{R}^n : (x-c)^{\mathrm{T}}\mathfrak{C}^{-1}(x-c) \leqslant 1\right\} \tag{31}$$

where $c \in \mathbb{R}^n$ is the center of the ellipsoid, and the matrix $\mathfrak{C} \in \mathbb{R}^{n\times n}$ characterizes the shape of the ellipsoid.

Assumption 1: The initial states $x_{i,0}$ of all agents satisfy the following constraint:

$$\Psi_0 \triangleq (x_{i,0} - \bar{x}_0)^{\mathrm{T}} P_0^{-1}(x_{i,0} - \bar{x}_0) \leqslant 1 \tag{32}$$

where P_0 is a known positive definite matrix.

The consensus control objective of the MASs is that all agents can have their states constrained within the given ellipsoid range with a probability no less than $\mathbf{p}$, that is, $x_{i,k}$ satisfies the following probabilistic ellipsoid constraint:

$$\mathbb{P}\left\{x_{i,k} \in \mathcal{Q}(\bar{x}_k, \Lambda_k)\right\} \geqslant \mathbf{p} \tag{33}$$

or

$$\mathbb{P}\left\{(x_{i,k} - \bar{x}_k)^{\mathrm{T}}\Lambda_k^{-1}(x_{i,k} - \bar{x}_k) \leqslant 1\right\} \geqslant \mathbf{p} \tag{34}$$

where $0 < \mathbf{p} < 1$ is a given probability value, and $\Lambda_k > 0$ is a given constraint matrix.

3. Main Results

In this section, sufficient conditions to ensure that the MAS (1) can achieve the consensus control objective (33) will be presented.

First, based on the consensus control objective (33), the following probability-guaranteed lemma holds.

Lemma 2: If $\Psi_k \triangleq \mathbb{E}\left\{(x_{i,k}-\bar{x}_k)^{\mathrm{T}}P_k^{-1}(x_{i,k}-\bar{x}_k)\right\} \leqslant 1$, then the following inequality holds:

$$\mathbb{P}\left\{x_{i,k} \in \mathcal{Q}(\bar{x}_k, \Lambda_k)\right\} \geqslant \mathbf{p} \tag{35}$$

where,

$$P_k \triangleq \frac{1}{1-\mathbf{p}}\Lambda_k. \tag{36}$$

3.1. Consensus Analysis

Define the following matrices:

$$\begin{aligned}
&\Theta_{\iota,i} \triangleq \big[\underbrace{0 \ \cdots \ 0}_{i-1} \ I_\iota \ \underbrace{0 \ \cdots \ 0}_{N-i}\big], \ \iota = \{n,m,q,w,v\},\\
&y_k \triangleq \mathrm{col}_N\{y_{i,k}\}, \ v_k \triangleq \mathrm{col}_N\{v_{i,k}\}, \ \tilde{C}_k \triangleq I_N \otimes C_k,\\
&e_k \triangleq \mathrm{col}_N\{e_{i,k}\}, \ \gamma_k \triangleq \mathrm{col}_N\{\gamma_{i,k}\}, \ \tilde{P} \triangleq \mathrm{diag}_N\{\bar{p}_i I_m\},\\
&\mathcal{R} \triangleq I_N - \tfrac{1}{N}\mathbf{1}_N\mathbf{1}_N^{\mathrm{T}}, \ \mathcal{F}_k \triangleq -2\tilde{P}((\mathcal{R}\mathfrak{H}\mathbf{1}_N^{\mathrm{T}}) \otimes (\tilde{K}_k T_1 C_k)),\\
&\mathcal{C}_k \triangleq I_N \otimes (A_k L_k) + \mathcal{H} \otimes (\tilde{K}_k T_1 C_k L_k) - 2\tilde{P}((\mathcal{R}\mathfrak{H}) \otimes (\tilde{K}_k T_1 C_k L_k)),\\
&\mathcal{T}_k \triangleq (2\tilde{P}-1)((\mathcal{R}\mathfrak{H}) \otimes \tilde{K}_k), \ \mathcal{S}_k \triangleq \mathcal{H} \otimes \tilde{K}_k - 2\tilde{P}((\mathcal{R}\mathfrak{H}) \otimes \tilde{K}_k),\\
&\mathcal{U}_k \triangleq (\mathcal{R}\mathfrak{H}) \otimes \tilde{K}_k, \ \mathcal{E}_k \triangleq \mathcal{H} \otimes (\tilde{K}_k E_k) - 2\tilde{P}((\mathcal{R}\mathfrak{H}) \otimes (\tilde{K}_k E_k)).
\end{aligned}$$

Theorem 1: Consider the MAS (1) under the encoding-decoding mechanism, given a sequence of positive definite matrices $\{P_k\}_{k\geqslant 0}$. If there exist non-negative scalars $\left\{\sigma_{i,k}^{(1)},\sigma_{i,k}^{(2)},\sigma_{i,k}^{(3)},\sigma_{i,k}^{(4)},\sigma_{i,k}^{(5)},\sigma_{i,k}^{(6)},\sigma_k^{(7)}\right\}_{k\geqslant 0}$ and real matrices $\{K_k\}_{k\geqslant 0}$ $(i \in \mathfrak{V})$ that satisfy

$$\begin{bmatrix} -\Phi_k & \varphi_k^{\mathrm{T}}\Theta_{n,i}^{\mathrm{T}} \\ \varphi_k\Theta_{n,i} & -P_{k+1} \end{bmatrix} \leqslant 0 \tag{37}$$

where

$$\begin{aligned}
&\Phi_k \triangleq \mathrm{diag}\{1,0,0,0,0,0,0,0\} + \sum_{i=1}^{N}\big(\sigma_{i,k}^{(1)}\Pi_{i,k}^{(1)} + \sigma_{i,k}^{(2)}\Pi_{i,k}^{(2)} + \sigma_{i,k}^{(3)}\Pi_{i,k}^{(3)} + \sigma_{i,k}^{(4)}\Pi_{i,k}^{(4)}\\
&\quad + \sigma_{i,k}^{(5)}\bar{W}_{i,k} + \sigma_{i,k}^{(6)}\bar{V}_{i,k}\big) + \sigma_k^{(7)}(\mathrm{diag}\{0,0,0,0,0,0,0,I_{nN}\} - \aleph_k^T\aleph_k),\\
&\Pi_{i,k}^{(1)} \triangleq \mathrm{diag}\{-1,\Theta_{q,i}^{\mathrm{T}}\Theta_{q,i},0,0,0,0,0,0\},\\
&\bar{\Pi}_{i,k}^{(2)} \triangleq [-(\mathbf{1}_N \otimes (TC_k))\bar{x}_k \ \ -(I_N \otimes (TC_kL_k))],\\
&\Pi_{i,k}^{(3)} \triangleq \mathrm{diag}\{-1,0,0,\frac{\alpha_i^2}{mM_i^2}\Theta_{w,i}^{\mathrm{T}}\Theta_{w,i},0,0,0\},\\
&\Pi_{i,k}^{(4)} \triangleq \mathrm{diag}\{-1,0,0,0,\frac{1}{m\lambda_i}\Theta_{w,i}^{\mathrm{T}}\Theta_{w,i},0,0,0\},\\
&\bar{W}_{i,k} \triangleq \mathrm{diag}\{-1,0,0,0,\Theta_{w,i}^{\mathrm{T}}W_{i,k}^{-1}\Theta_{w,i},0,0\},\\
&\bar{V}_{i,k} \triangleq \mathrm{diag}\{-1,0,0,0,0,0,\Theta_{v,i}^{\mathrm{T}}V_{i,k}^{-1}\Theta_{v,i},0\},\\
&\aleph_k \triangleq [\bar{\Gamma}_k(\mathbf{1}_N \otimes I_n)\bar{x}_k \ \ \bar{\Gamma}_k(I_N \otimes L_k) \ \ 0 \ \ 0 \ \ 0 \ \ 0],\\
&\tilde{\Gamma}_k \triangleq \bar{\Gamma}_k^T\bar{\Gamma}_k, \ \ \tilde{\Gamma}_k \triangleq \mathrm{diag}_N\Big\{\sum_{l=1}^{s}\Gamma_{il}\mathrm{tr}[\Omega_{il}]\Big\},\\
&\Pi_{i,k}^{(2)} \triangleq \frac{1}{2}\begin{bmatrix} 0 & * & * \\ \bar{\Pi}_{i,k}^{(2)} & 2I_{mN} & * \\ 0 & 0 & 0 \end{bmatrix},
\end{aligned} \tag{38}$$

L_k is a decomposition matrix of P_k, i.e., $P_k = L_kL_k^{\mathrm{T}}$. Then, the MAS can achieve the consensus control objective (33).

Proof: First, based on (26) and (27), we can obtain

$$\begin{aligned}\chi_{i,k} &= \sum_{j=1}^{N} h_{ij}(\hat{y}_{j,k} - y_{i,k}) \\ &= \sum_{j=1}^{N} h_{ij}((1-2\bar{p}_j)Q(y_{j,k}) + \gamma_{j,k} - y_{i,k}) \\ &= \sum_{j=1}^{N} h_{ij}((1-2\bar{p}_j)(y_{j,k} - e_{j,k}) + \gamma_{j,k} - y_{i,k}) \\ &= \sum_{j=1}^{N} h_{ij}(y_{j,k} - y_{i,k}) - 2\bar{p}_j \sum_{j=1}^{N} h_{ij} y_{j,k} + (2\bar{p}_j - 1)\sum_{j=1}^{N} h_{ij} e_{j,k} + \sum_{j=1}^{N} h_{ij}\gamma_{j,k}.\end{aligned} \tag{39}$$

The above Equation can be further expressed as

$$\begin{aligned}\chi_k &= (\mathcal{H}\otimes I_m - 2\tilde{P}(\mathfrak{H}\otimes I_m))y_k + (2\tilde{P}-1)(\mathfrak{H}\otimes I_m)e_k + (\mathfrak{H}\otimes I_m)\gamma_k \\ &= (\mathcal{H}\otimes I_m - 2\tilde{P}(\mathfrak{H}\otimes I_m))((I_N\otimes(T_1C_k))x_k + h_k + (I_N\otimes E_k)v_k) \\ &\quad +(2\tilde{P}-1)(\mathfrak{H}\otimes I_m)e_k + (\mathfrak{H}\otimes I_m)\gamma_k \\ &= ((\mathcal{H}\otimes(T_1C_k)) - 2\tilde{P}(\mathfrak{H}\otimes(T_1C_k)))x_k + (\mathcal{H}\otimes I_m - 2\tilde{P}(\mathfrak{H}\otimes I_m))h_k \\ &\quad +(\mathcal{H}\otimes E_k - 2\tilde{P}(\mathfrak{H}\otimes E_k))v_k + (2\tilde{P}-1)(\mathfrak{H}\otimes I_m)e_k + (\mathfrak{H}\otimes I_m)\gamma_k.\end{aligned} \tag{40}$$

Define the difference between the state $x_{i,k}$ and the average state $\bar{x}_k$ as

$$\begin{aligned}\tilde{x}_{i,k} &\triangleq x_{i,k} - \bar{x}_k, \\ \tilde{x}_k &\triangleq \mathrm{col}_N\{\tilde{x}_{i,k}\}.\end{aligned} \tag{41}$$

According to (28), (30), (40) and (41), we obtain

$$\begin{aligned}\tilde{x}_{k+1} &= x_{k+1} - (\mathbf{1}_N\otimes I_n)\bar{x}_{k+1} \\ &= \tilde{A}_k x_k + f_k + \tilde{B}_k\chi_k + \mathcal{D}_k\omega_k - (\mathbf{1}_N\otimes I_n)A_k\bar{x}_k - \frac{1}{N}(\mathbf{1}_N\mathbf{1}_N^{\mathrm{T}}\otimes\tilde{K}_k)\chi_k \\ &= (\tilde{A}_k + \mathcal{H}\otimes(\tilde{K}_kT_1C_k) - 2\tilde{P}((\mathcal{R}\mathfrak{H})\otimes(\tilde{K}_kT_1C_k)))x_k + \mathcal{S}_k h_k + \mathcal{E}_k v_k \\ &\quad +\mathcal{T}_k e_k + \mathcal{U}_k\gamma_k + \mathcal{D}_k\omega_k + f_k - (\mathbf{1}_N\otimes I_n)A_k\bar{x}_k.\end{aligned} \tag{42}$$

The proof of Theorem 1 will proceed by mathematical induction.

First, when $k=0$, we have $\Psi_0 \leqslant 1$ by Assumption 1.

Next, assume that for $k>0$, $\Psi_k \leqslant 1$ holds. We are going to prove that $\Psi_{k+1}\leqslant 1$ also holds under this assumption.

It is known that

$$\mathbb{E}\{(x_{i,k}-\bar{x}_k)^{\mathrm{T}}P_k^{-1}(x_{i,k}-\bar{x}_k)\} \leqslant 1, \tag{43}$$

is satisfied, then there exists $z_{i,k}\in\mathbb{R}^q$ such that $\mathbb{E}\{z_{i,k}^{\mathrm{T}}z_{i,k}\}\leqslant 1$, and

$$x_{i,k} = \bar{x}_k + L_k z_{i,k}. \tag{44}$$

Let $z_k \triangleq \mathrm{col}_N\{z_{i,k}\}$. Combining (44), we get

$$x_k = (\mathbf{1}_N\otimes I_n)\bar{x}_k + (I_N\otimes L_k)z_k. \tag{45}$$

Substituting (45) into (42), we can obtain

$$\begin{aligned}\tilde{x}_{k+1} &= (\mathbf{1}_N\otimes A_k - 2\tilde{P}((\mathcal{R}\mathfrak{H}\mathbf{1}_N^{\mathrm{T}})\otimes(\tilde{K}_kT_1C_k)))\bar{x}_k + (I_N\otimes(A_kL_k) \\ &\quad +\mathcal{H}\otimes(\tilde{K}_kT_1C_kL_k) - 2\tilde{P}((\mathcal{R}\mathfrak{H})\otimes(\tilde{K}_kT_1C_kL_k)))z_k + \mathcal{S}_k h_k \\ &\quad +\mathcal{E}_k v_k + \mathcal{T}_k e_k + \mathcal{U}_k\gamma_k + \mathcal{D}_k\omega_k + f_k - (\mathbf{1}_N\otimes I_n)A_k\bar{x}_k \\ &= -2\tilde{P}((\mathcal{R}\mathfrak{H}\mathbf{1}_N^{\mathrm{T}})\otimes(\tilde{K}_kT_1C_k))\bar{x}_k + (I_N\otimes(A_kL_k) + \mathcal{H}\otimes(\tilde{K}_kT_1C_kL_k) \\ &\quad -2\tilde{P}((\mathcal{R}\mathfrak{H})\otimes(\tilde{K}_kT_1C_kL_k)))z_k + \mathcal{S}_k h_k + \mathcal{E}_k v_k + \mathcal{T}_k e_k + \mathcal{U}_k\gamma_k \\ &\quad +\mathcal{D}_k\omega_k + f_k.\end{aligned} \tag{46}$$

Denote:

$$\zeta_k \triangleq [1 \;\; z_k^{\mathrm{T}} \;\; h_k^{\mathrm{T}} \;\; e_k^{\mathrm{T}} \;\; \gamma_k^{\mathrm{T}} \;\; \omega_k^{\mathrm{T}} \;\; v_k^{\mathrm{T}} \;\; f_k^{\mathrm{T}}]^{\mathrm{T}}, \tag{47}$$

$$\varphi_k \triangleq [\mathcal{F}_k\bar{x}_k \;\; \mathcal{C}_k \;\; \mathcal{S}_k \;\; \mathcal{T}_k \;\; \mathcal{U}_k \;\; \mathcal{D}_k \;\; \mathcal{E}_k \;\; I_{nN}]. \tag{48}$$

Then, (46) can be represented by the following Equation:

$$\tilde{x}_{k+1} = \varphi_k \zeta_k. \tag{49}$$

Substituting the above Equation, we can get

$$\begin{aligned} &\mathbb{E}\{\tilde{x}_{i,k+1}^{\mathrm{T}} P_{k+1}^{-1} \tilde{x}_{i,k+1}\} \\ &= \mathbb{E}\{\tilde{x}_{k+1}^{\mathrm{T}} \Theta_{n,i}^{\mathrm{T}} P_{k+1}^{-1} \Theta_{n,i} \tilde{x}_{k+1}\} \\ &= \mathbb{E}\{\zeta_k^{\mathrm{T}} \varphi_k^{\mathrm{T}} \Theta_{n,i}^{\mathrm{T}} P_{k+1}^{-1} \Theta_{n,i} \varphi_k \zeta_k\} \\ &\triangleq \mathbb{E}\{\zeta_k^{\mathrm{T}} \Upsilon_{i,k} \zeta_k\}. \end{aligned} \tag{50}$$

It is also known that the following inequality holds:

$$\begin{aligned} \mathbb{E}\{z_{i,k}^{\mathrm{T}} z_{i,k}\} &\leqslant 1, \\ \mathbb{E}\{\omega_{i,k}^{\mathrm{T}} W_{i,k}^{-1} \omega_{i,k}\} &\leqslant 1, \\ \mathbb{E}\{v_{i,k}^{\mathrm{T}} W_{i,k}^{-1} v_{i,k}\} &\leqslant 1. \end{aligned} \tag{51}$$

According to Lemma 2, we can further conclude that

$$\begin{aligned} \mathbb{E}\{\zeta_k^{\mathrm{T}} \Pi_{i,k}^{(1)} \zeta_k\} &\leqslant 0, \\ \mathbb{E}\{\zeta_k^{\mathrm{T}} \bar{W}_{i,k} \zeta_k\} &\leqslant 0, \\ \mathbb{E}\{\zeta_k^{\mathrm{T}} \bar{V}_{i,k} \zeta_k\} &\leqslant 0 \end{aligned} \tag{52}$$

where $\Pi_{i,k}^{(1)}$, $\bar{W}_{i,k}$, and $\bar{V}_{i,k}$ are defined in (38).

The inequality (7) can be transformed into the following form:

$$(I_{mN} h_k)^{\mathrm{T}} \left(h_k - (I_N \otimes (TC_k)) x_k\right) \leqslant 0. \tag{53}$$

Substituting (45) into (54), we get

$$h_k^{\mathrm{T}} I_{mN} \left(h_k - (\mathbf{1}_N \otimes (TC_k)) \bar{x}_k - (I_N \otimes TC_k L_k) z_k\right) \leqslant 0. \tag{54}$$

That is,

$$\mathbb{E}\{\zeta_k^{\mathrm{T}} \Pi_{i,k}^{(2)} \zeta_k\} \leqslant 0 \tag{55}$$

where $\Pi_{i,k}^{(2)}$ is defined in (38).

From (11) and the statistical properties of $\gamma_{i,k}$, we can obtain

$$\begin{aligned} e_{i,k}^{\mathrm{T}} e_{i,k} &\leqslant \frac{m M_i^2}{\alpha_i^2}, \\ \gamma_{i,k}^{\mathrm{T}} \gamma_{i,k} &\leqslant m \lambda_i. \end{aligned} \tag{56}$$

Thus, we have

$$\mathbb{E}\{\zeta_k^{\mathrm{T}} \Pi_{i,k}^{(3)} \zeta_k\} \leqslant 0, \tag{57}$$

$$\mathbb{E}\{\zeta_k^{\mathrm{T}} \Pi_{i,k}^{(4)} \zeta_k\} \leqslant 0 \tag{58}$$

where $\Pi_{i,k}^{(3)}$ and $\Pi_{i,k}^{(4)}$ are defined in (38).

From (2), we get

$$\mathbb{E}\{f_k^T f_k\} = \mathbb{E}\{\mathrm{tr}[f_k f_k^T]\} \leqslant \mathbb{E}\{x_k^T \tilde{\Gamma}_k x_k\} = \mathbb{E}\{\zeta_k^T \aleph_k^T \aleph_k \zeta_k\} \tag{59}$$

where $\tilde{\Gamma}_k$ and $\aleph_k$ are defined in (38). Then, the following inequality holds:

$$\mathbb{E}\left\{\zeta_k^T (\mathrm{diag}\{0,0,0,0,0,0,0,I_{nN}\} - \aleph_k^T \aleph_k) \zeta_k\right\} \leqslant 0 \tag{60}$$

According to [1], if there exist non-negative scalars $\left\{\sigma_{i,k}^{(1)}, \sigma_{i,k}^{(2)}, \sigma_{i,k}^{(3)}, \sigma_{i,k}^{(4)}, \sigma_{i,k}^{(5)}, \sigma_{i,k}^{(6)}, \sigma_k^{(7)}\right\}_{k \geqslant 0}$ that satisfy:

$$\begin{aligned} &\Upsilon_{i,k} - \mathrm{diag}\{1,0,0,0,0,0,0,0\} - \sum_{i=1}^{N} \left(\sigma_{i,k}^{(1)} \Pi_{i,k}^{(1)} + \sigma_{i,k}^{(2)} \Pi_{i,k}^{(2)} + \sigma_{i,k}^{(3)} \Pi_{i,k}^{(3)} + \sigma_{i,k}^{(4)} \Pi_{i,k}^{(4)}\right. \\ &\left. + \sigma_{i,k}^{(5)} \bar{W}_{i,k} + \sigma_{i,k}^{(6)} \bar{V}_{i,k}\right) - \sigma_k^{(7)} (\mathrm{diag}\{0,0,0,0,0,0,0,I_{nN}\} - \aleph_k^T \aleph_k) \leqslant 0, \end{aligned} \tag{61}$$

Then, the following inequality holds:

$$\zeta_k^{\mathrm{T}}\left(\Upsilon_{i,k}-\mathrm{diag}\{1,0,0,0,0,0,0,0\}\right)\zeta_k\leqslant 0. \tag{62}$$

Inequality (37) holds if and only if inequality (61) holds. Based on inequality (62), we can derive that

$$\begin{aligned}&\mathbb{E}\{\zeta_k^{\mathrm{T}}\varphi_k^T\Theta_{n,i}^{\mathrm{T}}P_{k+1}^{-1}\Theta_{n,i}\varphi_k\zeta_k\}-\zeta_k^{\mathrm{T}}\mathrm{diag}\{1,0,0,0,0,0,0,0\}\zeta_k\\&=\mathbb{E}\{\tilde{x}_{i,k+1}^{\mathrm{T}}P_{k+1}^{-1}\tilde{x}_{i,k+1}\}-\zeta_k^{\mathrm{T}}\mathrm{diag}\{1,0,0,0,0,0,0,0\}\zeta_k\leqslant 0,\end{aligned} \tag{63}$$

Thus, the following inequality holds:

$$\mathbb{E}\{\tilde{x}_{i,k+1}^{\mathrm{T}}P_{k+1}^{-1}\tilde{x}_{i,k+1}\}\leqslant 1. \tag{64}$$

That is,

$$\Psi_{k+1}\leqslant 1. \tag{65}$$

The proof is complete now. ■

3.2. Controller Design

In this subsection, we will provide sufficient conditions for the solvability of the proposed consensus control problem. The corresponding controller gains can be obtained by solving the recursive matrix inequality group in Theorem 2, whose proof is easily accessible from Theorem 1 and Lemma 2.

Theorem 2: Given the matrix sequence $\{\Lambda_k\}_{k\geqslant 0}$ and $0<\mathbf{p}<1$, if there exist non-negative scalars $\left\{\sigma_{i,k}^{(1)},\sigma_{i,k}^{(2)},\sigma_{i,k}^{(3)},\sigma_{i,k}^{(4)},\sigma_{i,k}^{(5)},\sigma_{i,k}^{(6)},\sigma_k^{(7)}\right\}_{k\geqslant 0}$ and real-valued matrices $\{K_k\}_{k\geqslant 0}$ that satisfy:

$$\begin{bmatrix}-\Phi_k & \varphi_k^{\mathrm{T}}\Theta_{n,i}^{\mathrm{T}}\\ \varphi_k\Theta_{n,i} & -\dfrac{1}{1-\mathbf{p}}\Lambda_{k+1}\end{bmatrix}\leqslant 0 \tag{66}$$

then the consensus control objective (33) is achieved.

4. Simulation Example

In this section, a specific simulation example is used to verify the effectiveness of the presented control algorithm. The relevant parameters of the multi-agent system are as follows:

$$\begin{aligned}&A_k=\begin{bmatrix}0.7+0.7e^{-k-1} & 0.2+0.1\sin(k+3)\\ 0.3+0.2\cos(k) & 0.8+0.03\cos(2k)\end{bmatrix},\ B_k=\begin{bmatrix}0.05\\0.03\end{bmatrix},\\&C_k=\begin{bmatrix}0.4+0.02\cos(k+4) & 0.6+0.1\sin(k+5)\end{bmatrix},\\&D_k=\begin{bmatrix}0.15\\0.45+0.03\sin(4k)\end{bmatrix},\ E_k=0.5,\ \mathfrak{M}_i=10,\\&f(x_{i,k})=\begin{bmatrix}0.01\\0.02\end{bmatrix}\left(3\varrho_{i,k}^{(1)}x_{i,k}^{(1)}+2\varrho_{i,k}^{(2)}x_{i,k}^{(2)}\right),\ W_{i,k}=1,\ V_{i,k}=1.\end{aligned}$$

where, $\varrho_{i,k}^{(1)}$ and $\varrho_{i,k}^{(2)}$ are uncorrelated Gaussian white noise sequences with zero mean and unit variance, $x_{i,k}^{(1)}$ and $x_{i,k}^{(2)}$ represent the first and second components of the agent state $x_{i,k}$, respectively.

The adjacency matrix of the topology graph is

$$\mathfrak{H}=\begin{bmatrix}0&1&1&1\\1&0&1&1\\1&1&0&1\\1&1&1&0\end{bmatrix}.$$

Set $\mathbf{p}=0.8$. The initial states of each agent are as follows:

$$\begin{aligned}&x_{1,0}=\begin{bmatrix}4\\-1\end{bmatrix},\ x_{2,0}=\begin{bmatrix}3\\1\end{bmatrix},\ x_{3,0}=\begin{bmatrix}1\\3\end{bmatrix},\\&x_{4,0}=\begin{bmatrix}-2\\2\end{bmatrix},\ P_0=\begin{bmatrix}27.82&-15.72\\-15.72&36.33\end{bmatrix}.\end{aligned}$$

It is obvious that the initial state of the system satisfies Assumption 1.The data payload of the binary codeword for agent i consists of $X_i=4$ bits, and the probability of a bit flip for each bit in the codeword is $\bar{p}_i=0.1$. The upper bound of the quantization range of the quantizer $Q_i(\cdot)$ is $M_i=48$, and the number of quantization levels is $\alpha_i=16$.

The simulation results are shown in Figures 3–7. Figure 7 illustrates the instances when the codewords of each

agent experience bit flips. Figures 3–4 respectively show the trajectories of $x_{i,k}$ (i.e., $x_{i,k}^{(1)}$ and $x_{i,k}^{(2)}$) and their state averages $\bar{x}_k$ (i.e., $\bar{x}_k^{(1)}$ and $\bar{x}_k^{(2)}$). It can be observed from the figures that the state trajectories of each agent converge towards the state average $\bar{x}_k$. Moreover, Figures 5–6 respectively depict the trends of the consensus errors $\tilde{x}_{i,k}$ (i.e., $\tilde{x}_{i,k}^{(1)}$ and $\tilde{x}_{i,k}^{(2)}$). It is evident that over time, $\tilde{x}_{i,k}$ fluctuates around 0. The simulation results indicate that under the bit flips, the designed algorithm can effectively ensure the consensus control performance of the system.

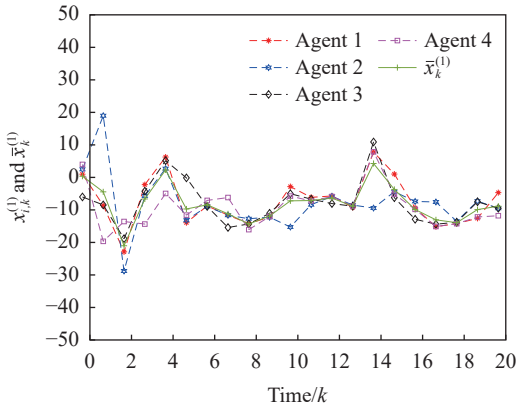

Figure 3. Trajectories of $x_{i,k}^{(1)}$ and $\bar{x}_k^{(1)}$.

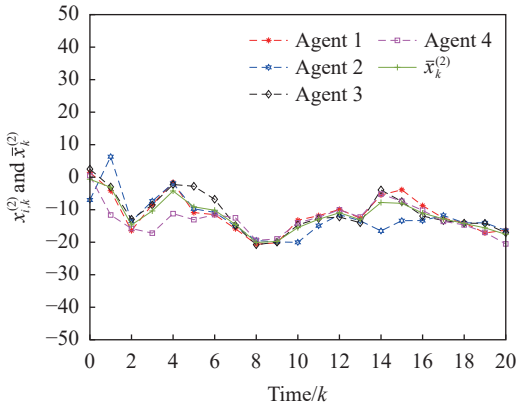

Figure 4. Trajectories of $x_{i,k}^{(2)}$ and $\bar{x}_k^{(2)}$.

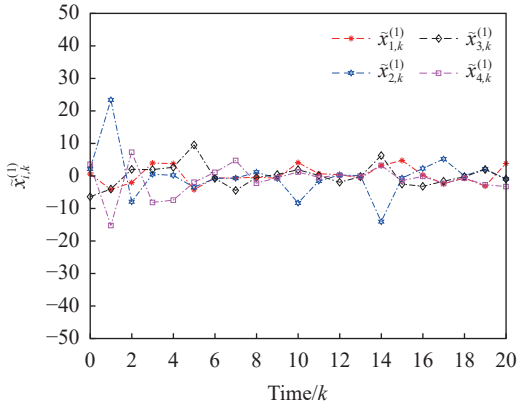

Figure 5. Trajectory of $\tilde{x}_{i,k}^{(1)}$.

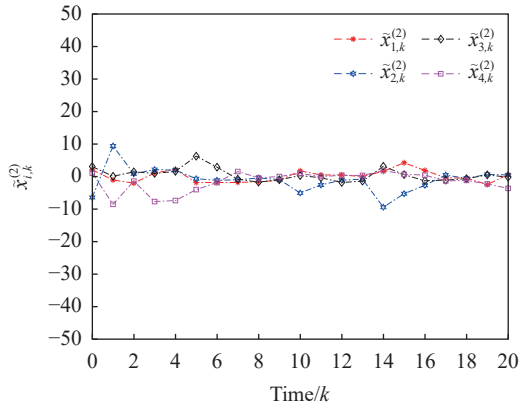

Figure 6. Trajectory of $\tilde{x}_{i,k}^{(2)}$.

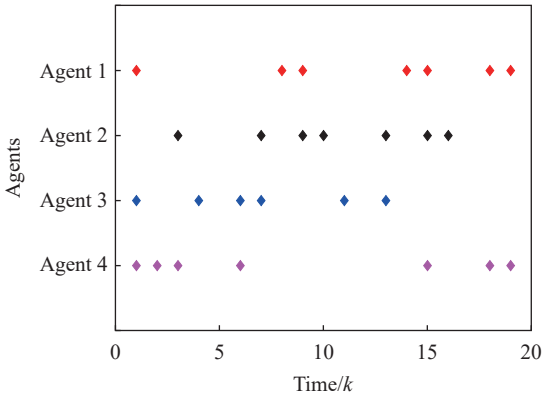

Figure 7. Instances of Bit Flips.

5. Conclusion

This paper investigates the probability-guaranteed consensus control problem of the time-varying MAS under bit flips. The impact of bit flips on the encoding-decoding mechanism under the bit-rate constraint is analyzed through stochastic analysis methods. Key contributions include modeling bit errors in quantization-based communication, transforming sensor saturation into sector-bounded nonlinearities, and deriving sufficient conditions for consensus via Lyapunov-based analysis. Future work could extend the framework to accommodate switching topologies, time-varying bit error rates, or adaptive quantization strategies, further enhancing its practical relevance in real-world networked control systems.

Author Contributions: **Shuo Yuan:** Writing - original draft, Validation, Software, Methodology, Conceptualization. **Lifeng Ma:** Supervision, Funding acquisition. **Chen Gao:** Writing - review & editing, Supervision, Methodology.

Funding: This work was supported in part by the National Natural Science Foundation of China under Grants 62273180 and 62403245, and the Natural Science Foundation of Jiangsu Province of China under Grants BK20241458 and BK20232038.

Data Availability Statement: Not applicable.

Conflicts of Interest: The authors declare no conflict of interest.

References

1. van den Broek, B.; Wiegerinck, W.; Kappen, B. Graphical model inference in optimal control of stochastic multi-agent systems. J. Artif. Intell. Res., **2008**, *32*: 95−122. doi: 10.1613/jair.2473
2. Cai, Y.Y.; Yang, X.B.; Yang, Y.; *et al*. Leader-following privacy-preserving consensus control of nonlinear multi-agent systems: A state decomposition approach. Int. J. Syst. Sci., **2025**, *56*: 2284−2295. doi: 10.1080/00207721.2024.2445726
3. Ding, L.; Han, Q.L.; Ge, X.H.; *et al*. An overview of recent advances in event-triggered consensus of multiagent systems. IEEE Trans. Cybern., **2018**, *48*: 1110−1123. doi: 10.1109/TCYB.2017.2771560

4. Wang, W.; Ma, L.F.; Rui, Q.Q.; *et al*. A survey on privacy-preserving control and filtering of networked control systems. Int. J. Syst. Sci., **2024**, *55*: 2269−2288. doi: 10.1080/00207721.2024.2343734
5. Guo, J.F.; Qian, W.; Wu, Y.M. Consensus of second-order multi-agent systems based on PIDD-like control protocol with time delay. Neurocomputing, **2025**, *618*: 129072. doi: 10.1016/j.neucom.2024.129072
6. Li, H.F.; Li, M. A time-varying gain method to consensus control of high-order nonlinear multi-agent systems with input saturations. Int. J. Syst. Sci., **2025**, *56*: 2357−2369. doi: 10.1080/00207721.2024.2447881
7. Ma, L.F.; Wang, Z.D.; Han, Q.L.; *et al*. Consensus control of stochastic multi-agent systems: A survey. Sci. China Inf. Sci., **2017**, *60*: 120201. doi: 10.1007/s11432-017-9169-4
8. Zhang, C.J.; Ji, L.H.; Yang, S.S.; *et al*. Data-driven distributed output consensus control for multi-agent systems with unknown internal state. Neurocomputing, **2025**, *615*: 128868. doi: 10.1016/j.neucom.2024.128868
9. Zou, L.; Liu, X.B.; Zhang, X.Y.; *et al*. Resilient consensus for multi-agent systems under distributed denial-of-service attacks: A graph-based approach. *J. Control Decis*. **2024**, in press. doi: 10.1080/23307706.2024.2442464.
10. Wang, B.C.; Zhang, J.F. Distributed output feedback control of Markov jump multi-agent systems. Automatica, **2013**, *49*: 1397−1402. doi: 10.1016/j.automatica.2013.01.063
11. Yu, W.W.; Ren, W.; Zheng, W.X.; *et al*. Distributed control gains design for consensus in multi-agent systems with second-order nonlinear dynamics. Automatica, **2013**, *49*: 2107−2115. doi: 10.1016/j.automatica.2013.03.005
12. Kang, L.F.; Ji, Z.J.; Liu, Y.G.; *et al*. Consensus of stochastic multi-agent systems with time-delay and Markov jump. Int. J. Syst. Sci., **2024**, *55*: 1959−1979. doi: 10.1080/00207721.2024.2328073
13. Ma, Y.Z.; Dong, X.X. Leader-following mean square consensus of stochastic switched multi-agent systems with event-triggered control. Int. J. Syst. Sci., **2024**, *55*: 2036−2049. doi: 10.1080/00207721.2024.2328785
14. Zhao, N.; Zhan, X.S.; Wu, J.; *et al*. Guaranteed-performance consensus control for multi-agent systems with external disturbances via event-triggered strategy. Neurocomputing, **2024**, *574*: 127268. doi: 10.1016/j.neucom.2024.127268
15. Han, F.; Liu, J.H.; Li, J.H.; *et al*. Consensus control for multi-rate multi-agent systems with fading measurements: The dynamic event-triggered case. Syst. Sci. Control Eng., **2023**, *11*: 2158959. doi: 10.1080/21642583.2022.2158959
16. Li, W.Q.; Xie, L.H.; Zhang, J.F. Containment control of leader-following multi-agent systems with Markovian switching network topologies and measurement noises. Automatica, **2015**, *51*: 263−267. doi: 10.1016/j.automatica.2014.10.070
17. Chen, J.C.; Sun, Q.; Shi, Y. Stochastic self-triggered MPC for linear constrained systems under additive uncertainty and chance constraints. Inf. Sci., **2018**, *459*: 198−210. doi: 10.1016/j.ins.2018.05.021
18. Muntwiler, S.; Wabersich, K.P.; Hewing, L.; *et al*. Data-driven distributed stochastic model predictive control with closed-loop chance constraint satisfaction. In *Proceedings of 2021 European Control Conference (ECC)*, *Delft*, *Netherlands*, *29 June–2 July 2021*; IEEE: New York, 2021; pp. 210–215. doi: 10.23919/ECC54610.2021.9655214.
19. Coulson, J.; Lygeros, J.; Dorfler, F. Distributionally robust chance constrained data-enabled predictive control. IEEE Trans. Automat. Contr., **2022**, *67*: 3289−3304. doi: 10.1109/TAC.2021.3097706
20. Zhang, W.J.; Liang, Y.; Wang, B.C. Differentially private coordination of second-order multi-agent systems via dynamic encoding-decoding. In *Proceedings of the 40th Chinese Control Conference (CCC)*, *Shanghai*, *China*, *26–28 July 2021*; IEEE: New York, 2021; pp. 5332–5337. doi: 10.23919/CCC52363.2021.9550215.
21. Meng, Y.; Li, T.; Zhang, J.F. Output feedback quantized observer-based synchronization of linear multi-agent systems over jointly connected topologies. Int. J. Robust Nonlinear Control, **2016**, *26*: 2378−2400. doi: 10.1002/rnc.3453
22. Wu, J.; Li, H.Q.; Han, Q.; *et al*. Leader-following consensus of nonlinear discrete-time multi-agent systems with limited bandwidth and switching topologies. ISA Transactions, **2020**, *99*: 139−147. doi: 10.1016/j.isatra.2019.10.002

Citation: Yuan, S.; Ma, L.; Gao, C. Probability-Guaranteed Consensus Control for Nonlinear Multi-Agent Systems Under Bit Flips. *International Journal of Network Dynamics and Intelligence*. 2025, 4(3), 100020. doi: 10.53941/ijndi.2025.100020